J|A|C|S ARTICLES

Published on Web 07/24/2009

# Primary Role of the Electrostatic Contributions in a Rational Growth of Hysteresis Loop in Spin-Crossover Fe(II) Complexes

Mikaël Kepenekian,[†,‡] Boris Le Guennic,[†] and Vincent Robert*[,†]

*Université de Lyon Laboratoire de Chimie, Ecole Normale Supérieure de Lyon, CNRS, 46 allée d'Italie, F-69364 Lyon, France, and Laboratoire de Reconnaissance Ionique et de Chimie de Coordination, CEA-INAC/LCIB (UMRE 3 CEA-UJF), 17 rue des Martyrs, F-38054 Grenoble Cedex 9, France*

Received April 21, 2009; Revised Manuscript Received July 3, 2009; E-mail: vincent.robert@ens-lyon.fr

***Abstract:*** We report a comprehensive analysis of the hysteresis behavior in a series of well-characterized spin-crossover Fe(II) materials. On the basis of the available X-ray data and multireference CASSCF (complete active space self-consistent field) calculations, we show that the growth of the hysteresis loop is controlled by electrostatic contributions. These environment effects turn out to be deeply modified as the crystal structure changes along the spin transition. Our theoretical inspection demonstrates the synergy between weak bonds and electrostatic interactions in the growth of hysteresis behavior. Quantitatively, it is suggested that the electrostatic contributions significantly enhance the cooperativity factor while weak bonds are determinant in the structuration of the 3D networks. Our picture does not rely on any parametrization but uses the microscopic information to derive an expression for the cooperativity parameter. The calculated values are in very good agreement with the experimental observations. Such inspection can thus be carried out to anticipate the hysteresis behavior of this intriguing class of materials.

## 1. Introduction

The constant development and characterization of sophisticated materials holding switchable physical properties stems from their possible applications to electronic devices such as thermal sensors, optical switches, and information storage media.[1,2] A prerequisite to generate memory effects is the presence of bistable units within the crystal structure. Striking examples are to be found in spin-crossover (SCO) Fe(II) complexes, such as **1** = [Fe(pm-pea)$(NCS)_2$] (pm-pea = *N*-2′-pyridylmethylene-4-(phenylethynyl)aniline) and analogues **2** = [Fe(pm-bia)-$(NCS)_2$] (pm-bia = *N*-2′-pyridylmethylene-amino-biphenyl) and **3** = [Fe(pm-aza)-$(NCS)_2$] (pm-aza = *N*-2′-pyridylmethylene-4-(phenylazo)aniline) (see Figure 1).[3−6] In such materials, the transition occurs between a low-spin state (LS, $S = 0$) and a high-spin state (HS, $S = 2$). While compounds **1**, **2**, and **3** belong to the same family characterized by a $N_6$ coordination sphere, hysteretic behavior has been recently reported in other environments such as $N_4O_2$.[7−10] In particular, compound **4** = [Fe(3-MeO,5-$NO_2$-sal-N(1,4,7,10))] was fully characterized and exhibits a LS to HS transition.[9]

Over the past decade, much effort has been dedicated to the synthesis of cooperative materials to grow thermal hysteresis, using not only covalent linkers to form coordination polymers[1,11−13] but also van der Waals interactions between the transiting units. In spite of promising results,[1] such as the possibility to photoinduce reversible spin transition[14] with attractive applications in multilayer materials,[15] the former strategy has not led to the expected breakthroughs in the generation of large hysteresis loops at room temperature. An alternative route consists in the establishment of communication networks to generate supramolecular interactions through extended aromatic structures held by the ligands. $\pi$-Stacking is indeed considered to play a crucial

[†] Ecole Normale Supérieure de Lyon.
[‡] CEA-INAC/LCIB.

(1) Kahn, O.; Martinez, C. J. *Science* **1998**, *279*, 44–48.
(2) Létard, J.-F.; Guionneau, P.; Goux-Capes, L. *Top. Curr. Chem.* **2004**, *235*, 221–249.
(3) Létard, J.-F.; Guionneau, P.; Codjovi, E.; Lavastre, O.; Bravic, G.; Chasseau, D.; Kahn, O. *J. Am. Chem. Soc.* **1997**, *119*, 10861–10862.
(4) Guionneau, P.; Le Gac, F.; Lakhoufi, S.; Kaiba, A.; Chasseau, D.; Létard, J.-F.; Négrier, P.; Mondieig, D.; Howard, J. A. K.; Léger, J.-M. *J. Phys.: Condens. Matter* **2007**, *19*, 326211.
(5) Létard, J.-F.; Guionneau, P.; Rabardel, L.; Howard, J. A. K.; Goeta, A. E.; Chasseau, D.; Kahn, O. *Inorg. Chem.* **1998**, *37*, 4432–4441.
(6) Guionneau, P.; Létard, J.-F.; Yufit, D. S.; Chasseau, D.; Bravic, G.; Goeta, A. E.; Howard, J. A. K.; Kahn, O. *J. Mater. Chem.* **1999**, *9*, 985–994.
(7) Weber, B.; Kaps, E.; Weigan, J.; Carbonera, C.; Létard, J.-F.; Acheterhold, K.; Parak, F. G. *Inorg. Chem.* **2008**, *47*, 487–496.
(8) Weber, B.; Bauer, W.; Obel, J. *Angew. Chem., Int. Ed.* **2008**, *47*, 10098–10101.
(9) Salmon, L.; Bousseksou, A.; Donnadieu, B.; Tuchagues, J.-P. *Inorg. Chem.* **2005**, *44*, 1763–1773.
(10) Weber, B. *Coord. Chem. Rev.* **2008**, doi 10.1016/j.ccr.2008.10.002.
(11) Garcia, Y.; Niel, V.; Munoz, M. C.; Real, J. A. *Top. Curr. Chem.* **2004**, *233*, 229–257.
(12) Matouzenko, G. S.; Molnar, G.; Bréfuel, N.; Perrin, M.; Bousseksou, A.; Borshch, S. A. *Chem. Mater.* **2003**, *15*, 550–556.
(13) Matouzenko, G. S.; Perrin, M.; Le Guennic, B.; Genre, C.; Molnar, G.; Bousseksou, A.; Borshch, S. A. *Dalton Trans.* **2007**, 934–942.
(14) Bonhommeau, S.; Molnar, G.; Galet, A.; Zwick, A.; Real, J.-A.; McGarvey, J. J.; Bousseksou, A. *Angew. Chem., Int. Ed.* **2005**, *44*, 4069–4073.
(15) Cobo, S.; Molnar, G.; Real, J. A.; Bousseksou, A. *Angew. Chem., Int. Ed.* **2006**, *45*, 5786–5789.

 **10.1021/ja9031677 CCC: $40.75** 

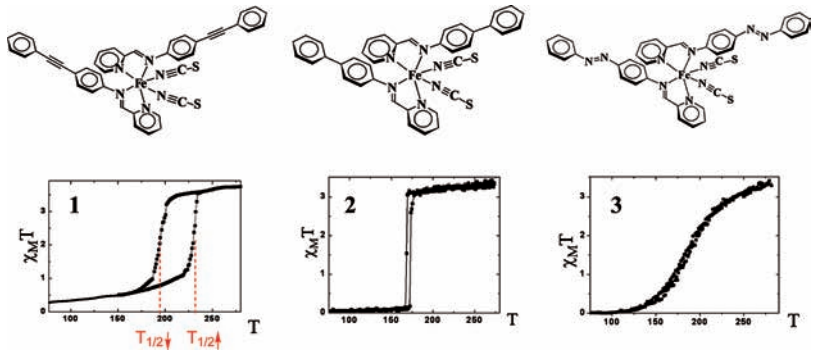


***Figure 1.*** Molecular units of Fe(II)$N_6$ SCO compounds under investigation (top). Despite similarities, the cooperativity manifestation distinguishes compounds **1**, **2**, and **3** [$\chi_M T$ ($cm^3 \cdot K \cdot mol^{-1}$) vs $T$ (K) plots, bottom].[6] Reproduced by permission of the Royal Society of Chemistry.

role in growing spectacular hysteresis loops characterized by thermal widths $\Delta T = T_{1/2\uparrow} - T_{1/2\downarrow}$ (see Figure 1) up to 92 K.[3,16]

In the meantime, the need for interpretations has stimulated intense theoretical developments.[17−21] While the regular solution-based theories introduce an intermolecular energy contribution (so-called elastic interactions), the physical origin is mainly attributed to the ∼0.20 Å Fe−N bond distance change. In the model proposed by Slichter and Drickamer,[22] an interaction term $\Gamma x(1 - x)$ is added to the Gibbs free energy $G$, where $x$ stands for the HS molar fraction.[23] $\Gamma$ is a phenomenological interaction parameter which is assumed to be temperature-independent. Within this mean-field model, a cooperativity parameter has been defined with respect to the average transition temperature $T_{1/2}$, $C = \Gamma/2RT_{1/2}$.[24] Since $C$ values larger than unity are required, one can expect a memory effect around room temperature (i.e., $RT_{1/2} \sim 300$ K) for $\Gamma \sim 600$ K. Besides, the larger the value of $C$, the wider the hysteresis loop.[23] To complement the use of van der Waals weak bonds as intermolecular contacts, H-bonds have been considered to ever enhance the cooperativity in materials preparation.[9] Interestingly, the destruction of the H-bond network has been invoked to account for a significant reduction of the hysteresis loop observed in the [FeL(imidazole)$_2$] compound (L being a tetradentate $N_2O_2^{2-}$ Schiff-base-like ligand).[25] The apparent need for such large intermolecular interactions called for particular synthetic strategies we would like to comment on. Even though most of the spin transiting systems consist of Fe(II)$N_6$ cores, the electronic densities[26,27] and three-dimensional organizations significantly differ from one to another in the LS to HS regimes. Indeed, the importance of packing effects has been remarkably demonstrated in the polymorphs class of Fe(dppa)$(NCS)_2$ [dppa = (3-aminopropyl)bis(2-pyridylmethyl)amine] complex.[28] While polymorph C in ref 28 exhibits a 8 K hysteresis loop, the phenomenon is suppressed in polymorph A. To our knowledge, however, much rationalization and interpretation arise from weak bonds networks analysis, whereas there is little concern for the purely electrostatic-origin mechanism, as summarized in a Madelung field picture.

In the present work, we report a comprehensive analysis of the hysteresis behavior in Fe(II) materials resulting from the structure-induced changes of electrostatic contributions along the transition. Using the information extracted from ab initio multireference CASSCF (complete active space self-consistent field) calculations[26,27] and experimental observations,[29] it is demonstrated that such fluctuations allow for (i) a hysteresis loop evaluation and (ii) a microscopic understanding of the memory effect establishment. Based upon the LS and HS X-ray structures of a series of synthetic Fe(II)$N_6$ compounds **1**, **2**, and **3**, we offer an expression and evaluation of the intermolecular parameter $\Gamma$. To this purpose, the intermolecular interactions are split and evaluated as the traditionally discussed van der Waals ($\Gamma_{vdW}$) contribution and a subsequent polarizing term attributed to the crystal organization ($\Gamma_{pol}$). We finally suggest that weak bonds might be of prime importance to organize specific three-dimensional networks whereas the resulting crystal structures induce specific electrostatic contributions which play a determinant role in hysteresis loop growth. Our approach based upon ab initio calculations is predictive since the computed intermolecular parameter $\Gamma$ values agree with the experimentally observed reduction of $\Delta T$ from **1** to **3**. To further validate our strategy by including chemical changes in the Fe(II) coordination sphere, similar calculations were performed upon **4** to evaluate $\Gamma$ and support the small hysteretic behavior in a prototype Fe(II)$N_4O_2$ compound.

## 2. Computational Details

CASSCF calculations were performed upon the isolated basic units of **1**, **2**, **3**, and **4**. Such methodology working with the exact Hamiltonian is known to provide satisfactory description of electronic structures, a major concern in our approach. A limited number of electrons distributed over a set of valence molecular orbitals (MOs) define the active space (CAS). As reported in the literature,[26,30−32] the standard CAS consists of (i) the mainly Fe 3d character orbitals extended with a set of virtual orbitals of the

(16) Létard, J.-F.; Capes, L.; Chastanet, G.; Moliner, N.; Létard, S.; Real, J. A.; Kahn, O. *Chem. Phys. Lett.* **1999**, *313*, 115–120.
(17) Wajnflasz, J. *Phys. Status Solidi* **1970**, *40*, 537.
(18) Bari, R. A.; Sivardière, J. *Phys. Rev. B* **1972**, *5*, 4466–4471.
(19) Zimmermann, R.; König, E. *J. Phys. Chem. Solids* **1977**, *38*, 779.
(20) Nishino, M.; Boukheddaden, K.; Konishi, Y.; Miyashita, S. *Phys. Rev. Lett.* **2007**, *98*, 247203.
(21) Sasaki, N.; Kambara, T. *J. Phys. Soc. Jpn.* **1987**, *56*, 3956.
(22) Slichter, C. P.; Drickamer, H. G. *J. Chem. Phys.* **1972**, *56*, 2142–2160.
(23) Bolvin, H.; Kahn, O. *Chem. Phys.* **1995**, *192*, 295–305.
(24) Purcell, K. F.; Edwards, M. P. *Inorg. Chem.* **1984**, *23*, 2620–2625.
(25) Jäger, E. G. In *Chemistry at the Beginning of the Third Millenium*; Fabrizzi, L., Poggi, A., Eds.; Springer: Berlin, 2000.
(26) Kepenekian, M.; Robert, V.; Le Guennic, B.; de Graaf, C. *J. Comput. Chem.* **2009**, doi 10.1002/jcc.21236 (published online).
(27) Kepenekian, M.; Le Guennic, B.; Robert, V. *Phys. Rev. B* **2009**, *79*, 094428.
(28) Matouzenko, G. S.; Bousseksou, A.; Lecocq, S.; van Koningsbruggen, P. J.; Perrin, M.; Kahn, O.; Collet, A. *Inorg. Chem.* **1997**, *36*, 5869–5879.
(29) Legrand, V.; Pillet, S.; Souhassou, M.; Lugan, N.; Lecomte, C. *J. Am. Chem. Soc.* **2006**, *128*, 13921–13931.
(30) Bolvin, H. *J. Phys. Chem. A* **1998**, *102*, 7525–7534.

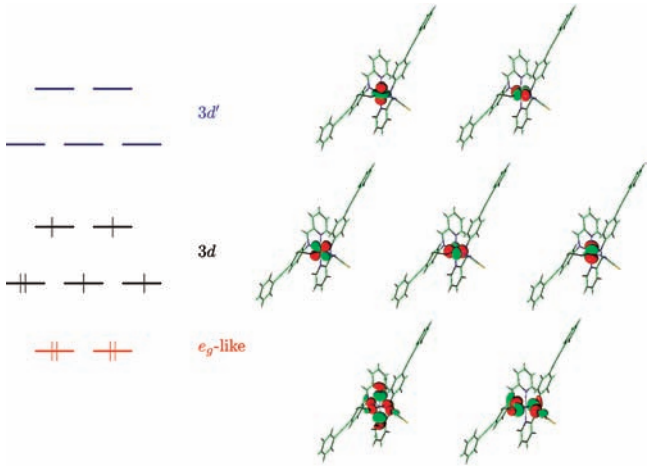


***Figure 2.*** CAS[10,12] active space and selected "$e_g$-like" and 3d localized active orbitals for complex **1**.

same symmetry (so-called 3d′ orbitals) and (ii) two occupied "$e_g$-like" symmetry orbitals with mainly ligand character. Thus, a CAS[10,12] including 10 electrons in 12 active orbitals (see Figure 2) is used in the calculations.

The valence MOs were then relocalized into atomic-like orbitals to grasp the importance of the charge transfer (CT) contributions accessible in the wave function expansion. This transformation leaves any observable expectation value unchanged and affords a valence-bond (VB) type analysis.[33,34] In particular, one can evaluate the amplitudes of the different electronic configurations and derive atomic properties such as charges. All our calculations were performed with the Molcas7.0 package[35] including atomic natural orbitals (ANO-RCC) as basis sets.[36,37] As stated previously,[26] finely balanced basis sets are necessary to properly describe the energetics of the SCO phenomenon. Thus, a [7s6p5d3f2g1h] contraction was used for Fe, whereas the contractions [3s2p1d], [4s3p1d], [4s3p1d], [3s3p1d], and [1s] were used for C, N, O, S, and H, respectively.

## 3. Results and Discussion

The search for cooperativity has led to intense experimental works to control the weak interactions (i.e., van der Waals) in chemical engineering strategies. Let us first concentrate on the Fe(II)$N_6$ series, namely compounds **1**, **2**, and **3**. By use of the recent LS and HS crystal structure determinations of **1** ($2RT_{1/2}$ = 425 K),[3,4] $\pi$-stacking interactions can be evaluated from accurate ab initio calculations.[38] The resulting "like-spin" $E_{LS,LS}$, $E_{HS,HS}$ and "unlike-spin" $E_{LS,HS}$ energies give access to the intermolecular parameter based upon the van der Waals contribution $\Gamma = \Gamma_{vdW}$ as $(2E_{LS,HS} - E_{LS,LS} - E_{HS,HS}) \sim 115$ K. Along this framework, the cooperativity factor in **1** is $C = 0.27$, a value that is incompatible with the existence of a thermal hysteresis ~40 K.[3] The analogues **2** and **3** exhibit much smaller hysteresis widths supported by variations in the three-dimensional arrangements, $\pi-\pi$ stackings, and carbon−sulfur contacts. Indeed, **2** undergoes an abrupt transition with a sharp hysteresis (5 K) around 170 K,[5] whereas **3** shows a very gradual spin conversion with no clear hysteresis (see Figure 1).[6,39] Thus, one may wonder how much the simultaneous (i) charge redistribution upon the basic units (i.e., ligand field), (ii) geometry reorganizations, and (iii) lattice expansion are likely to modulate the electrostatic contributions generated by the crystal environment (i.e., Madelung fields) along the transition.[26,27] Assuming the additivity of the resulting polarizing effects ($\Gamma_{pol}$) with the weak bond contacts ($\Gamma_{vdW}$), we first derived an expression for $\Gamma_{pol}$. Then the intermolecular cooperative parameter was calculated as $\Gamma = \Gamma_{vdW} + \Gamma_{pol}$.

***Table 1.*** Calculated Atomic Charges upon the Iron and Nitrogen Atoms and Average Potential Differences $\langle V_\alpha^{Fe} - V_\alpha^{X} \rangle$ in **1**[a]

| | $Q^{Fe}$ | $Q^{N}$ | $Q^{N'}$ | $\langle V_\alpha^{Fe} - V_\alpha^{X} \rangle$ |
|---|---|---|---|---|
| LS | 1.45 | −0.36 | −0.18 | $6.32 \times 10^{-5}$ |
| HS | 1.92 | −0.48 | −0.24 | $-2.14 \times 10^{-3}$ |

[a] α = HS, LS and X = N, N′, where N′ stands for the nitrogen atoms of the pm-pea ligand. Values are given in atomic units, au.

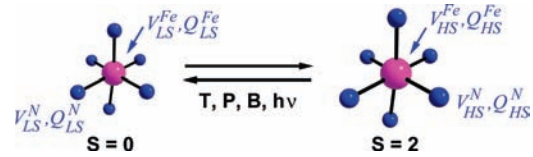


***Figure 3.*** Calculated charges and potentials generated by the rest of the transiting units in the crystal at the Fe and N positions are indicated as $Q_\alpha^X$ and $V_\alpha^X$ (α = HS, LS and X = Fe, N). A polarization of the Fe−N bonds is anticipated.

On the basis of relocalized MOs extracted from the CASSCF calculations, average charges upon the iron and nitrogen sites of the LS and HS basic unit of **1** were estimated (see Table 1 and Figure 3 for notations).[26,27] One should mention that the nitrogen atom of the thiocyanate group (N) hold a negative charge which is about as twice as large as that of the pm-pea ligand nitrogen atoms (N′).

From the low- and high-temperature X-ray data of **1**,[3,4] the LS and HS Madelung potentials were evaluated at the Fe, N, and N′ atomic positions by growing until convergence the crystal structure with the point charges given in Table 1. Interestingly, the average potentials difference $\delta V_{HS} = \langle V_{HS}^{Fe} - V_{HS}^{N} \rangle$ (see Figure 3 for notations) between the iron and nitrogen positions reaches ~ −700 K in the HS phase, a value which might greatly affect the intermolecular parameter Γ. As soon as the basic unit is immersed in the crystal structure, additional electrostatic contributions arising from these neighboring point charges located at the crystallographic positions must be taken into account. In the high-temperature phase, the on-site Fe and N potentials difference $\delta V_{HS}$ generated by the rest of the crystal units is likely to polarize the Fe−N bonds. Evidently, a similar phenomenon characterized by $\delta V_{LS}$ is active in the low-temperature regime. Quantitatively, a HS $FeN_6$ unit undergoes a supplementary mean Madelung potential arising from an $x/(1 - x)$ distribution of HS/LS sites:

(31) Fouqueau, A.; Casida, M. E.; Lawson Daku, L. M.; Hauser, A.; Neese, F. *J. Chem. Phys.* **2005**, *122*, 044110.
(32) Pierloot, K.; Vancoillie, S. *J. Chem. Phys.* **2006**, *125*, 124303.
(33) Sadoc, A.; Broer, R.; de Graaf, C. *J. Chem. Phys.* **2007**, *126*, 134709.
(34) Banse, F.; Girerd, J.-J.; Robert, V. *Eur. J. Inorg. Chem.* **2008**, 4786–4791.
(35) Karlström, G.; Lindh, R.; Malmqvist, P.-A.; Roos, B. O.; Ryde, U.; Veryazov, V.; Widmark, P.-O.; Cossi, M.; Schimmelpfennig, B.; Neogrady, P.; Seijo, L. *Comput. Mater. Sci.* **2003**, *28*, 222–239.
(36) Roos, B. O.; Lindh, R.; Malmqvist, P.-A.; Veryazov, V.; Widmark, P.-O. *J. Phys. Chem. A* **2004**, *108*, 2851–2858.
(37) Roos, B. O.; Lindh, R.; Malmqvist, P.-A.; Veryazov, V.; Widmark, P.-O. *J. Phys. Chem. A* **2005**, *109*, 6575–6579.
(38) Sinnokrot, M. O.; Sherrill, C. D. *J. Phys. Chem. A* **2006**, *110*, 10656–10668.
(39) Guionneau, P.; Marchivie, M.; Bravic, G.; Létard, J.-F.; Chasseau, D. *Top. Curr. Chem.* **2004**, *234*, 97–128.

$$Q^{Fe}_{HS}[xV^{Fe}_{HS} + (1 - x)V^{Fe}_{LS}] + \sum_{N6,core} Q^{N}_{HS}[xV^{N}_{HS} + (1 - x)V^{N}_{LS}]$$

while a similar expression holds for a LS unit. This particular contribution cannot be excluded a priori in the Gibbs energy. It has been shown[27] that both the charge redistribution $\Delta Q = Q^{Fe}_{HS} - Q^{Fe}_{LS}$ and polarization fluctuation $\delta V_{LS} - \delta V_{HS}$ accompanying the LS to HS change lead to an intermolecular contribution $\Gamma_{pol}x(1 - x)$ with

$$\Gamma_{pol} = \Delta Q(\delta V_{LS} - \delta V_{HS})$$

Not only is Slichter and Drickamer's expression recovered but a physical understanding of $\Gamma$ is suggested. Averaging over the 6 nonstrictly equivalent nitrogen positions (4 N and 2 N′), a mean $\delta V_{LS} - \delta V_{HS}$ value was calculated to be equal to 696 K (see Table 1). Since the charge redistribution $\Delta Q$ is 0.47 from Table 1, a $\Gamma_{pol} = 329$ K value is found in **1**. Therefore our construction based upon ab initio information leads to a cooperativity factor of 0.78, a value that stresses a propensity toward hysteresis behavior driven by the polarization effects.

As soon as both contributions are included, the intermolecular cooperative parameter can be calculated from $\Gamma = \Gamma_{vdW} + \Gamma_{pol} = 444$ K (see Table 2), leading to $C = 1.04$. Not only is this value consistent with the experimental observations upon **1** but it also demonstrates that rigorous ab initio calculations can give access to relevant ingredients for hysteresis understanding. Using precisely the same approach to evaluate both contributions in the analogues of **1**, we found that $\Gamma = 220$ K in **2** whereas $\Gamma$ is negligible in **3**. Our approach is effectively supported by experimental data[4] since the hysteresis loop is reduced in **2** and turns out to be almost negligible in **3**. From the literature,[6] the carbon−sulfur contacts, possibly among others, should not be discarded in this class of compounds but remain to be accurately quantified to fully recover the hysteretic behavior in **2**. Let us mention that a similar trend has been recently anticipated[27] in the polymorphs of Fe(dppa)$(NCS)_2$ compound.[28] Nevertheless, the lack of low-temperature X-ray data did not allow one to support this electrostatic-based analysis.

By changing the chemical environment of the Fe(II) center, the hysteretic behavior was also examined in the synthetic compound **4** (see Figure 4), a prototype Fe(II)$N_4O_2$ system exhibiting a hysteresis loop between 125 and 129 K.[9] Using the calculated atomic charges (see Table 3) and the available high- and low-temperatures X-ray data, the polarization effects account for $\Gamma_{pol} = 150$ K in **4**. Since the weak-bond contributions are expected to be very similar to the previous Fe(II)$N_6$ series, the cooperativity factor was calculated as 270 K (see Table 2). Thus, our determination of $\Gamma$ is suggestive of hysteretic behavior. This result is not only in agreement with experimental observations, but also supports the importance of the electrostatic contributions in Fe(II)$N_4O_2$ spin-transiting compounds.

Whatever the coordination sphere, this quantitative and predictive picture also offers a microscopic four-step scenario as depicted in Figure 5. As the LS Madelung field is turned on (step 1), the electronic distribution of the isolated units is modified as compared to the "gas phase". By raising the temperature, the elementary unit undergoes a LS → HS transition depicted by the coordination sphere expansion into a metastable state (step 2). Step 3 corresponds to the stabilization of the HS units as the Madelung field generated by the crystal environment is modified from LS to HS (i.e., fluctuation of polarization effects). The potential difference $\delta V_{HS} < 0$ greatly stabilizes the characteristic metal-to-ligand electron transfer. Then on cooling (step 4), the settled HS Madelung field blocks the electron flow from the N and N′ sites back to the Fe center within the Fe(II)$N_6$ core. This electron trapping phenomenon results in $T_{1/2\downarrow} < T_{1/2\uparrow}$.

With an ever-growing demand for wider hysteresis loops, we finally looked into some specific geometrical factors affecting

***Table 2.*** Calculated $\Gamma$ Values,[a] Experimental Hysteresis Widths $\Delta T$, and $2RT_{1/2}$ Values in Compounds **1**, **2**, **3**, and **4**

| | **1** | **2** | **3** | **4** |
|---|---|---|---|---|
| $2RT_{1/2}$ (K) | 425 | 340 | 380 | 250 |
| $\Delta T$ (K) | 40 | 5 | ∼0 | 4 |
| $\Gamma$ (K) | 444 | 220 | ∼0 | 270 |

[a] Calculated as $\Gamma = \Gamma_{pol} + \Gamma_{vdW}$.

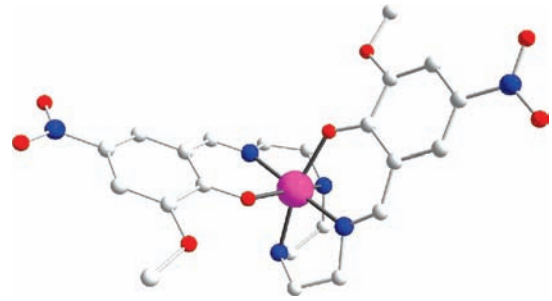

***Figure 4.*** [Fe(3-MeO,5-$NO_2$-sal-N(1,4,7,10))] compound (**4**). Fe, O, N, and C atoms are depicted in pink, red, blue, and gray, respectively. H atoms are not shown for clarity.[9]

***Table 3.*** Calculated Atomic Charges upon the Iron, Nitrogen, and Oxygen Atoms and Average Potential Differences in **4**[a]

| | $Q^{Fe}$ | $Q^{N}$ | $Q^{O}$ | $\langle V^{Fe}_{\alpha} - V^{X}_{\alpha}\rangle$ |
|---|---|---|---|---|
| LS | 1.48 | −0.19 | −0.36 | $3.43 \times 10^{-4}$ |
| HS | 1.90 | −0.25 | −0.45 | $-5.65 \times 10^{-4}$ |

[a] Values are given in atomic units, au.

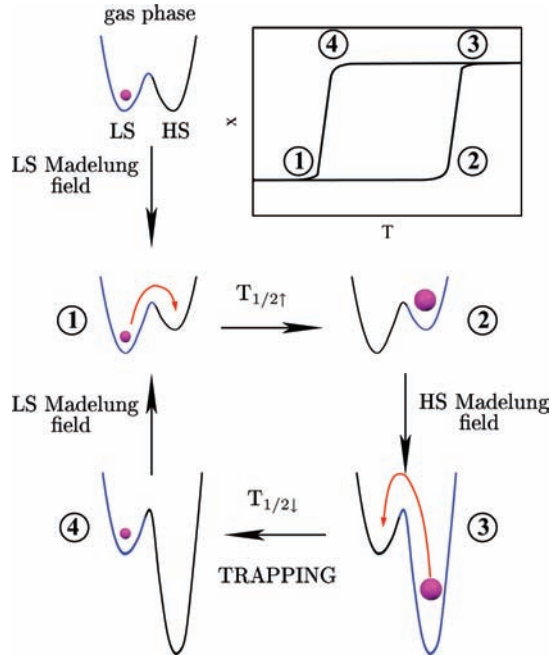


***Figure 5.*** Four-step scenario for the hysteresis loop opening. The Madelung field modifications along the transition differentiate the warming and cooling regimes.

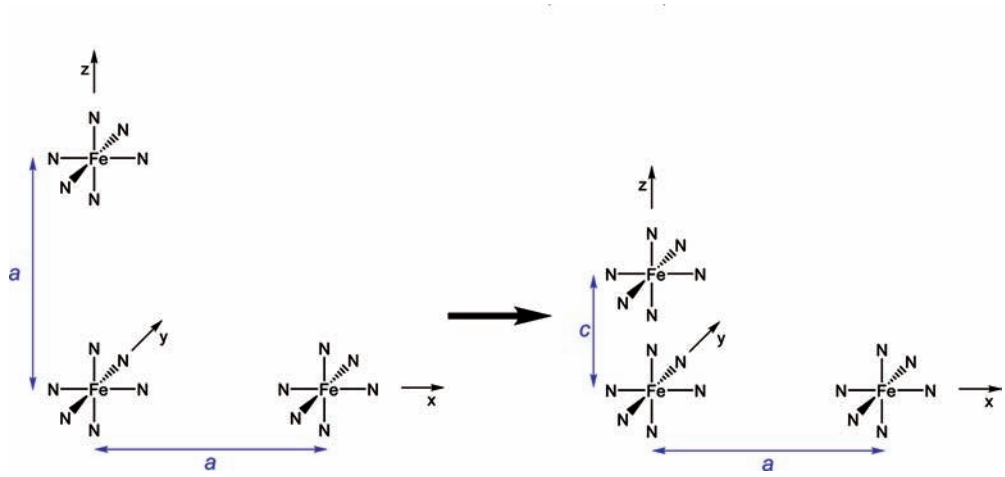


***Figure 6.*** Cubic to tetragonal lattice distortions in $[Fe(NCH)_6]^{2+}$. Counteranions are not represented for clarity.

***Table 4.*** Calculated $\Gamma_{pol}$ Values for "One-dimensional-like" and "Two-dimensional-like" Lattice Expansions along the Transition[a]

| LS | HS | $\Gamma_{pol}$ (K) |
|---|---|---|
| $a = b = c = 11.75$ | $a = b = c = 12.0$ | 750 |
| $a = b = 11.75$, $c = 11.5$ | $a = b = 11.75$, $c = 12.0$ | 470 |
| $a = b = 11.75$, $c = 11.5$ | $a = b = 12.0$, $c = 11.5$ | 3800 |

[a] Orthorhombic lattice parameters $a$, $b$, and $c$ are given in angstroms.

the cooperativity. Since the relative positions of the basic units seem to be of particular importance,[28] this specific issue was also examined using a bistable system of $O_h$ symmetry, namely $[Fe(NCH)_6]^{2+}$. This particular system has been much debated in the literature as a prototype bistable system.[26,27,30] Thus, the sensitivity of the memory effect with respect to the polarization contributions (i.e., $\Gamma_{pol}$) was assessed. Starting from a hypothetical cubic lattice, the Madelung field fluctuations were evaluated by allowing tetragonal disortions (Figure 6), featuring a typical 4% change of the unit cell volume as observed in SCO compounds. Indeed, anisotropic lattice disortions traditionally accompany the phase transition.

First, a reference $\Gamma_{pol}$ value (750 K in Table 4) was evaluated by considering a purely isotropic expansion of the cubic unit cell. Then different lattice expansions were examined starting from an orthorhombic structure, forcing a 4% change of the volume. From Table 4, the lattice expansion along one particular direction (i.e., "one-dimensional-like") slightly reduces the intermolecular interactions parameter calculated within our approach (470 vs 750 K). In contrast, a "two-dimensional-like" expansion is likely to greatly favor hysteresis behavior (3800 vs 750 K). Such observation might be of interest in the preparation of memory effect materials.

## 4. Conclusion

In conclusion, the available ab initio information upon the basic unit of SCO compounds sheds light on important charge reorganizations that induce significant Madelung potentials changes at a macroscopic level. Our inspection of $Fe(II)N_6$ synthetic systems demonstrates the synergy between weak bonds and electrostatic interactions in the growth of hysteresis loops. We believe that the prime role traditionally attributed to weak bonds in cooperativity phenomena should be reconsidered. Quantitatively, it is suggested that the electrostatic contributions significantly enhance the cooperativity factor ($\Gamma_{pol}/\Gamma \sim 0.74$ for compound **1**) while weak bonds are determinant in the structuring of three-dimensional networks. Our picture does not rely on any parametrization of the intermolecular interactions but uses the microscopic information to derive an expression for the cooperativity parameter. In the synthetic compound **1**, $\Gamma$ is found to be 444 K, a value that is consistent with the experimentally observed memory effect. Our microscopic analysis of the phenomenon holds for other coordination spheres such as $N_4O_2$, since a large contribution to the cooperativity factor arises from the electrostatic modulations ($\Gamma_{pol}/\Gamma \sim 0.56$ for compound **4**). We believe that such macroscopic description based on numerical electrostatic predictions complements the common phenomenological models for cooperativity[40] and thus should help the preparation of applied devices.

**Acknowledgment.** We thank Dr. G. Chastanet, O. Maury, and H. Bolvin for stimulating discussions and Dr. P. Guionneau and J.-F. Létard for providing us with X-ray crystallographic data and Figure 1, respectively. The research was supported by the ANR-07-JCJC-0045-01 (*fdp*-magnets) project.

JA9031677

(40) Spiering, H. *Top. Curr. Chem.* **2004**, *235*, 171–195.